MASTER'S THESIS

Master of Science in Advanced Mathematics and Mathematical Engineering

Title: Mathematical modeling of calcium handling dysfunctions leading to atrial fibrillation

Author: Nikolina Križanec

Advisor: Blas Echebarria Domínguez
Angelina Peñaranda Ayllon

Department: Facultat de Matematiques i Estadistica

Academic year: 2016/2017

UNIVERSITAT POLITÈCNICA DE CATALUNYA
BARCELONATECH
Facultat de Matemàtiques i Estadística

Universitat Politécnica de Catalunya
Facultat de Matemàtiques i Estadística

Master in Advanced Mathematics and Mathematical Engineering

Master's thesis

Mathematical modeling of calcium handling dysfunctions leading to atrial fibrillation

Nikolina Križanec

Supervised by

Blas Echebarria Domínguez and
Angelina Peñaranda Ayllon

3rd October 2017

Abstract

The aim of this master's thesis is to study the basic cardiac cellular electrophysiology in order to understand and examine the role of SK3 channels. Among the many channels present in an atrial myocyte, SK3 channels are activated by calcium, providing the circulation of the intracellular calcium. A well established mathematical model, the Grandi model, forms the basis of the simulations presented in this project.

First, to study the effect of the SK current, a modification of the atrial myocyte model is done. Secondly, the model is calibrated according to experimental results. Lastly, we study the effect of the SK currents to avoid spontaneous calcium release induced depolarizations.

Numerical simulations of the whole-cell atrial myocyte performed in this project confirmed the anti arrhythmic behaviour of the SK current, that counteracts the effect of spontaneous calcium release. This effect is, however, not large and, therefore, does not seem to support the, development of SK channel blockers as a new therapeutic strategy in the treatment of atrial fibrillation, as has been suggested in the literature.

Keywords: cardiac electrophysiology, SK channels, atrial fibrillation

Contents

1 Introduction

1.1 Anatomy of the heart

The heart is a muscular organ that acts as a bio-mechanical pump [1] and has a conical shape. It is located in the center of the chest, between the right and left lungs and protected by the rib cage. By the end of the average human lifetime it is recorded more than 5 billion heartbeats. Under normal conditions (siting, relaxing, no illness) the heart rate is normally between 60 and 100 beats per minute and each day the heart pumps about 7500 liters of blood. Two thirds of the heart's mass is found on the left part of the body; it is often said that the heart points left. A normal, healthy, adult heart usually is about the size of a clenched adult fist and it weights approximately 300 grams. In an average weighting adult the human heart is approximately 0.3 % of the total mass. Although a minuscule portion of a person's total weight, the heart plays one of the most important roles in the entire body.

The heart has four chambers; the two upper chambers are the right and left atria, while the two lower chambers are called right and left ventricles. The muscular wall that separates atria and ventricles is called septum. The atria are smaller compared to the ventricles and they have thinner muscular walls. The atria are directly connected to the veins that brings blood into the heart, so the atria are receiving chambers. The ventricles are the larger, stronger chambers connected to the arteries through which the blood is pumped out to the entire body.

Blood flow is regulated by the constantly opening and closing of the heart valves; tissue-paper thin membranes located on the heart wall. Valves are in charge of regulating the blood flow in only one direction throughout the heart. There exist two types of heart valves: atrioventricular and semilunar valves. The atrioventricular valves are located, as the name suggests, between the atria and ventricles and they regulate the flow from the atria to the ventricles. The second type of valves are located between the ventricles and aorta letting the blood to be carried out of the heart.

1.2 Basic cardiac cellular electrophysiology

Electrical impulses originating in specialized cells and caused by the flow of ions across the outer membrane give rise to a wave of excitation that spreads through the entire heart. This excitation wave initiates, and coordinates the contraction of the cardiac cells pumping blood to the body and to the heart itself. The electrical excitation of the heart is intimately linked to other processes that together constitute the "heart beat". This electrical excitation both initiates mechanical contraction through intracellular calcium release, and is itself influenced by the changing

geometry of the cells. A description of basic cardiac cellular electrophysiology is included in this section to provide a background to subsequent chapters.

Each cardiac muscle cell is encapsuled within a thin membrane. The outer membrane of the cardiac cell encapsules a small volume that is known as the intracellular space within which there is a compartment called sarcoplasmic reticulum (SR). The extracellular space is defined to be outside the membrane of the cell. In the cell membrane there are membrane-spanning proteins that combine to form small holes or pores, often referred to as ion channels. These channels allow only specific ions to pass through the membrane and only under certain conditions [1]. It is this property of selective permeability that allows electric potential differences to form between the inside and outside of the cell. The main ions that are of interest in cardiac electrophysiology are sodium, potassium and calcium. The two forces acting on these ions to create the potential difference across the cell membrane are a chemical force and an electrical force. When a concentration gradient of a particular ion species exists, the ions will naturally flow this concentration gradient to create an uniform solution. This movement then causes an electrical gradient to be established that opposes the chemical gradient. The potential at which the chemical and electrical forces acting on a single ion species are in equilibrium is called Nernst or reversal potential. The Nernst potential E_x of an ion x can be written as

$$E_x = \frac{RT}{z_x F} \log_e \frac{[x]_e}{[x]_i}$$

where R is the universal gas constant (8.314 $J\ mol^{-1}\ K^{-1}$), T is absolute temperature, z_x is the valence of the ion x and F is Faraday's constant (96 485 $C\ mol^{-1}$). $[x]_e$ and $[x]_i$ are the extracellular and intracellular concentrations of the ion x.

The potential difference across the cell membrane is known as the transmembrane potential V_m, given as a difference between the potential in the intracellular space and potential in extracellular space. Cardiac muscle cells have an inbuilt protection mechanism whereby a small pertubation in the potential difference across the cell membrane elicits only a passive response. From such a perturbation the transmembrane potential will move back towards the resting state. If a sufficiently large stimulus is given, however, the transmembrane potential will rise above a critical point known as the threshold potential and an active response, called action potential, will occur. A typical action potential from a cardiac muscle cell can be divided into four phases (see Figure 1).

At rest, the cell membrane is in a polarized state. The rise at the beginning of the action potential gets the transmembrane potential close to zero and this is therefore known as depolarization. When the cell recovers and the potential returns to a negative state the cell is said to be repolarized. If the membrane potential decreases to a point where it is below the cell's resting potential it is said to be hyperpolarized. The sharp upstroke at the start of the action potential is due to a rapid influx of sodium ions due to the sodium current I_{Na}. This

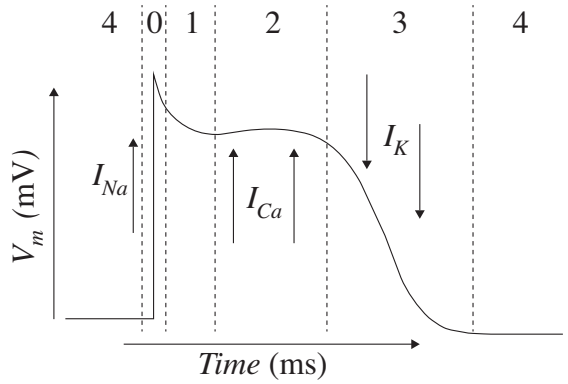

Figure 1: A typical action potential from a cardiac muscle cell can be divided into four phases delineated by dashed lines.

upstroke is known as phase 0 of the action potential. In phase 1 there is a rapid decrease in the membrane potential due to an outward potassium current. The existence and length of the relatively flat plateau in the action potential (phase 2) is due to inward currents I_{Ca} that are mainly based on the flow of calcium ions. Throughout the action potential there are potassium-based currents I_K that tend to bring the transmembrane potential back to the resting potential. In phase 3 the calcium currents cease to hold the membrane potential in a depolarized state and the potassium currents return the cell to a repolarized state (phase 4) which is close to the Nernst potential for potassium.

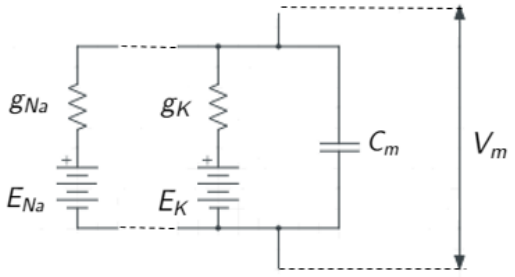

Figure 2: The electric circuit analogy that represent the flow of current across the cell membrane.

From an electrical perspective, the cell membrane acts as a capacitance in parallel with a series of resistors representing the ion channels in the membrane (see Figure 2). The direction of current flow across the cell membrane through each type of ion channel is governed by the difference between the transmembrane potential and the Nernst potential of that ion. This leads to the following expression for the

current through an arbitrary channel I_x:

$$I_x = g_x(V_m - E_x) \tag{1}$$

where E_x is the reversal potential for ion x and g_x is the conductance of the channel for that ion (conductance is the inverse of resistance R_x). The conductances are, in general, dependent both on time and on the transmembrane potential although in some cases they are also sensitive to the concentrations of specific ions. With the conductances arranged in parallel, the currents through each of the ion channesls may be summed linearly to give I_{ion}, which represents the total current flowing through the membrane;

$$I_{ion} = \sum_x I_x \tag{2}$$

With the advent of improved experimental techniques the number of different ion channels that have been identified continues to increase and, therefore, the representation of I_{ion} continues to become more complex but also more realistic. Placing this current in parallel to the current through the capacitive component of the membrane circuit yields the following expression for the total current flow I_m trough the membrane over time;

$$I_m = C_m \frac{dV_m}{dt} + I_{ion} = 0 \tag{3}$$

1.3 Contraction of the heart

In a typical human lifetime, the heart beats over 2 billion times. A heartbeat compiles a complex set of very accurate and harmonized repeated chain of events. Therefore, the contraction sequence of the heart follows a very specific model based on the two fundamental parts: diastole and systole. The phase of relaxation is called diastole and the phase of contraction is called systole. As mentioned before, the human heart is a four chambered organ; thus, there are atrial systole, atrial diastole, ventricular systole and ventricular diastole.

Atrial and ventricular diastole, often called the complete cardiac diastole, is a period of time when the atria and ventricles relax after contraction and are prepared to fill with blood. When the atrium fills with oxygen-poor blood from the vena cavae, the pressure opens the atriventricular valves and the blood drains into the ventricles. Contraction of the atria (atrial systole) fills the ventricles completely whereupon begin to relax. When ventricle fills with blood, it contracts (ventricular systole) and the increasing pressure forces the valves to open. Blood is forwarded into the big arteries leading away from the heart. Once the blood left the venticles, they start to relax. Oxygen-rich blood returns from the lungs to the atrium through the pulmonary veins and the whole process starts all over again.

1.3.1 Cardiac conduction system

Coordination of the contraction of the heart is fully assigned to the propagation of the cardiac action potential. At the molecular scale the spread of the action potential between adjacent cardiomyocytes is proceeded through gap junction. At the organ level the action potential is usually generated by the sinoatrial node. The sinoatrial node is directly connected to the atria and, through certain fibres, the action potential is quickly transferred from the right atrium to the left atrium. Then the impulse travels through internodal pathways in the right atrium reaching the atrioventricular node from where the action potential slowly spreads out to the ventricles. Cardiomyocytes known as Purkinje Fibers transmit the cardiac action potential with large speed throughout both ventricles. Afterwards, the signal travel down to the apex of the heart and then projects throughout the myocardium.

The total sequence of excitation is shown diagrammatically in Figure 3.

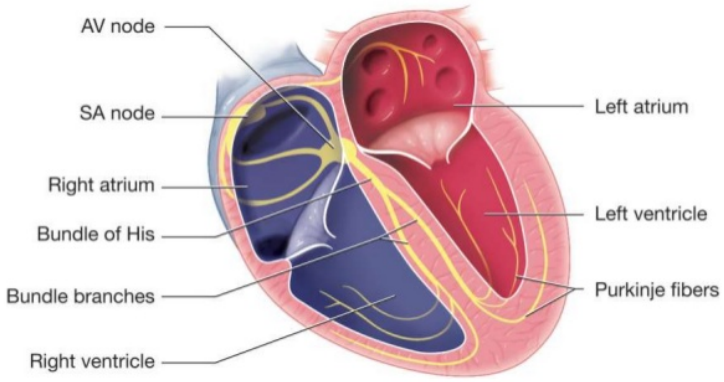

Figure 3: Simplified view of the cardiac excitation sequence. Figure reproduced from the on line version of the book 'Medical Language" 3rd edition by Susan M. Turley, 2014.

1.3.2 Calcium and contraction

As the action potential emanating from the sinoatrial node (SA) sweeps over the heart, it produces the depolarisation of the myocytes, causing them to contract. This process is known as excitation-contraction (EC) coupling [14]. Ca^{2+} is the link between myocyte depolarisation and contraction. It binds to troponin C within a complex of proteins that are associated with the thin (actin) filaments in myocytes. The binding of Ca^{2+} to troponin C displaces tropomyosin, and allows engagement of actin and myosin filaments. These myofilaments slide past each other and contract the cell. The simultaneous contraction of many cells within the atrial and ventricular walls generates sufficient force to propel blood around the

heart, lungs and body.

1.3.3 Ca^{2+} and cardiac excitation–contraction coupling

Excitation-contraction coupling represents the process by which an electrical action potential leads to contraction of cardiac muscle cells [19]. During the phase 2 of the action potential, when a myocyte is depolarized, calcium ions influx into the cell through L-type calcium (voltage-sensitive) channels which are located on the sarcolemma. Because the concentration of the calcium in intracelular space now is bigger than those in the extracellular space, this initial calcium influx triggers a consequent calcium release out of the concentrated storage in the sarcoplasmic reticulum. Calcium flows out of the SR through specific channels, known as ryanodine receptors and the reaction whereby calcium is able to activate this channel is called calcium-induced calcium release (CICR) proccess, see Figure 4. These large levels of intracellular calcium concentration act on tropomyosin complexes, that is two-stranded protein, to induce heart contraction.

When the phase 2 ends, the influx of calcium is slower and calcium is secluded by sarcoplasmic reticulum, precisely by the calcium pump called SERCA, accordingly decreasing the cytosolic calcium level. Transportation of the calcium out of the cell is governed by the sodium-calcium-exchange pump.

The crucial mediator of the excitation–contraction coupling during each action potential is calcium and its cycling in and out of the cytosol. There exists a well established relation between excitation of the cell, calcium flow and heart contraction. The strength of the current that is generated by the calcium-sodium exchanger affects the duration and form of the action potential. Given that the strenght of this current depends on the level of calcium in the intracellular space of cell, a feedback mechanism appears between the strength of the contraction, and corresponding calcium transient, and the duration of APD.

1.3.4 SCR and AF

Atrial fibrillation (AF) is the most common cardiac arrhythmia in humans; of hospitalizations associated with heart rhythm disturbances, approximately one-third is accounted for by AF. For the general population, the lifetime risk of developing AF is approximately 25% after the age of 40, with relative incidence increasing with age [8]. This pathology arises when electrical impulses do not solely arise from the sinoatrial node, but instead spontaneously occur with high frequency from sites around the atria. Although not devastating per se, AF is associated with reduced quality of life and increased risk of stroke. The latter is a consequence of compromised atrial contraction. In combination, this predisposes to thromboembolic stroke and heart failure (HF). Thromboembolism caused by stagnation of blood flow is

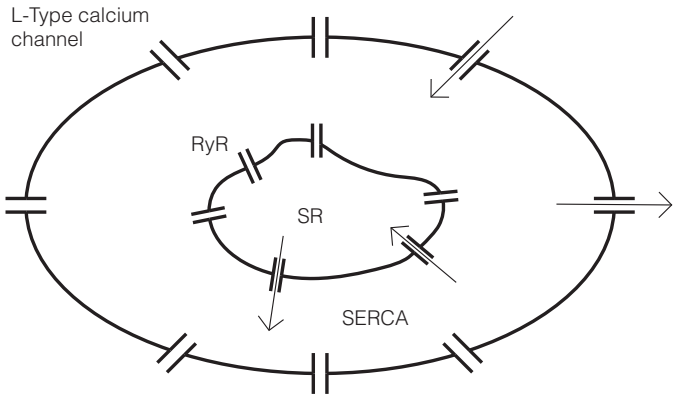

Figure 4: Calcium enters the cardiomyocyte via L-type calcium channels. Calcium then activates ryanodine receptors on the sarcoplasmic reticulum (SR). This special receptors senses intracellular calcium and trigger calcium release from the SR to further increase calcium availability in the cell. As the contraction ends, intracellular calcium returns to the SR via the SERCA calcium channel.

a significant complication arising from atrial fibrillation. It is therefore clear that co-ordinated atrial function is very important. Heart failure is a common cause of atrial fibrillation, atrial myocytes phenotypically remodel during the disease such that they have reduced contraction, and a greater propensity to show spontaneous Ca^{2+} signals. During the remodelling, atrial myocytes alter the expression of key proteins involved in Ca^{2+} homeostasis, storage and signal generation. Such changes unfortunately appear to reinforce the incidence of fibrillation.

In general, an anomalous spontaneous contraction, produced by the spontaneous calcium release, may produce an increase in the sodium-channel exchanger current. When this current is large enough, it can generate an early afterdepolarizations (EADs) or delayed afterdepolarizations (DADs) by opening the sodium channels. EADs and DADs, shown in the Figure 5, act as triggers for the generation of abnormal impulses. When afterdepolarizations are large enough to reach threshold, there appears the premature action potential, represented by dashed line. If the afterdepolarization shows up in the repolarizing phase 3 of the action potential it is called the early afterdepolarization, and if takes place in the phase 4 of action potential it is called delayed afterdepolarization.

1.4 Small-conductance Ca^{2+}-activated potassium (SK) channels

Gating is the mechanism of opening and closing of ion channels. Ion channels can be categorized by their mechanism of gating: voltage-dependent, ligand-dependent and mechano-sensitive gating. Voltage gated ion channels change their conductance due to voltage differences across the membrane.

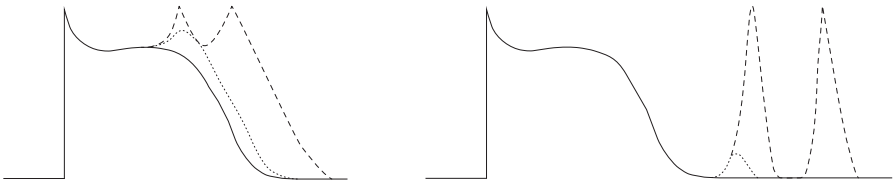

Figure 5: Figure representing the standard action potential (solid line), failed afterdepolarisation (dot-line) and afterdepolarization (dashed line). On the left figure, the dashed line represents EAD while on the right figure the DAD.

In this work we are interested in cardiac potassium channels. There exist three subcategories that potassium channels can be placed into: voltage-gated, inward rectified channels and background currents. Among the different potassium currents involved in the repolarisation phase, we will study a class of currents activated by Ca^{2+}. Their importance will be seen in relation to SCR.

Several recent studies imply that spontaneous Ca^{2+} release is necessary for the activation of the SK channels [26], [27]. Some authors demonstrate that generic ablation of the SK channels in mouse prolonged atrial APD, and increased appearance of EAD [28]. In addition, in the canine left atrium it is found that apamin stimulates arrhythmia. Therefore, some authors suggest that inhibition of the SK channels may lead to more heterogeneous APD change dispersion of repolarization [29].

The family of Ca^{2+}-activated K^+ channels has been divided into three classes based on their single channel conductance. Hence, the classes have been named big-conductance Ca^{2+}-activated potassium (BK) channels, intermediate-conductance Ca^{2+}-activated potassium (IK) channels and small-conductance Ca^{2+}-activated potassium (SK) channels. In this project we will focus on SK channels.

IK channels are not reported to be present in cardiac myocytes but play important roles in vessels as key players in blood pressure regulation. BK channels play an important role in intracellular compartments such as the mitochondria where they are involved in ischemia–reperfusion injuries. Within the family of Ca^{2+}-activated K^+ channels, it is however only the SK channels that seem to be functionally expressed in the plasma membrane of cardiomyocytes and thereby have the possibility to directly impact cardiac action potential morphology. SK channels are present in both atria and ventricles. However, the functional activation of SK channels and thereby their intrinsic impact on action potential generation are significantly more prominent in atria compared with ventricles. SK channels are blocked by apamin, a neurotoxin in bee venom [5]. The family of SK channels consists of three members with differential sensitivity to apamin: SK1 with the least sensitivity, SK2 with the highest sensitivity and SK3 with intermediate sensitivity.

As the name implies, small-conductance Ca^{2+}-activated potassium channels are

gated only by intracellular Ca^{2+}. Biophysically, SK channels are activated almost instantly by increases in intracellular Ca^{2+} with an activation being directly proportional to $[Ca^{2+}]_i$ and hence, provide a critical link between changes in intracellular Ca^{2+} and membrane potentials. In contrast, the deactivation rate is independent on $[Ca^{2+}]_i$.

SK channels were first discovered in skeletal muscle [15], and subsequently they have been found in a wide range of cell types: neuronal, endothelia, epithelia,... The idea of Ca^{2+}-activated potassium channels linking free intracellular Ca^{2+} to the opening of K^+ channels is not new and could explain a number of effects on transmembrane currents by free cytosolic Ca^{2+}. During the 1970s, numerous findings of supposed calcium activated potassium currents were made but however also rejected. It was not until 1999 that the first convincing evidence of cardiac calcium activated potassium channels was presented. In 2003, Xu et al [20] demonstrated apamin-sensitive current in atrial myocytes from both mice and men. The apamin-sensitive current was shown to be significantly larger in atrial myocytes compared with ventricular myocytes in mice line. In atria, there is ample evidence that SK channels contribute to action potential repolarization. Inhibition of SK currents has been shown to prolong APD in mouse and human atrial myocytes. Furthermore, ablation of SK2 channel resulted in a significant prolongation of APD in atrial myocytes while overexpression of SK3 showed a significant shortening of APD. All tree SK channel subtypes were found in mouse hearts by Chiamvimonvat et al [21] in 2005. The first indication that I_{SK} might play a role in AF was presented in 2007 in work by Ozgen et al [22] where fast pacing increased the presence of SK channels, as manifested in the APD abbreviation and the sensitivity of the current to apamin. In 2009, Chiamvimonvat et al [23] provided evidence of a more direct connection between I_{SK} and AF by showing that atrial cardiomyocytes from SK2 knock-out mice had prolonged atrial APD and early afterdepolarizations (EADs). The proarrhythmic effects in studies include prolonged atrial APD, increased occurrences of early after depolarization (EAD), increased APD heterogeneity, occurrences of electrical alternans, and wave breaks. Other works link this remodelling with chanced trafficking of SK channels to the membrane during rapid atrial tachycardia (that is a heart rate that exceeds the normal resting rate). There are, however, contradicting resuts: SK1 and SK2 channel expression as well as apamin-sensitive currents were significantly reduced in right atrial appendages recovered from chronic atrial fibrillation (AF) patients [9], while SK3 expression was down-regulated in patients with permanent atrial fibrillation [10]. Given this partially contradictory laboratory data, in 2010, Ellinor et al did genome-wide association studies, revealing that polymorphisms in the calcium-dependent potassium-channel gene KCNN3 are important risk factor for AF [16].

However, a clear framework for the different pro- or anti-arrhythmic effects of

inhibition of SK channel which could explain the different laboratory data and provide an explanation for the clear genome wide-association studies is lacking [2].

Little has been done regarding modeling of SK channels and the effect of Ca^{2+}-activated potassium channels in cardiac electrophysiology in order to understand or unveil different pro- or anti-arrhythmic effects of inhibition of SK channels. Recently, the effect of calcium-sensitive potassium currents on voltage and calcium alternans in a ventricular cell model has been studied but no similar study has been performed for atrial cell models. In this work we will investigate its effects on an atrial action potential model. Due to the lack of knowledge of the details of some key features of SK3, we will study its effects under different scenarios. This should be the starting point in order to test whether SK channels could avoid or limit the effect of spontaneous calcium release and contraction on the generation of EAD's.

1.5 Goals of the project

The general goal is to study the effect of SK currents in SCR induced depolarizations. For this, we will:

- Modify a well established atrial myocyte model to include the SK current
- Study the change of APD due to SK currents and calibrate the strength of this current comparing the results with experimental data
- Study the effect of SK current on depolarization, setting a fixed release of calcium at different times after repolarization

2 Methods

2.1 Model

As we already know, atrial fibrillation is the most common cardiac arrhythmia observed clinically. The underlying mechanism remains unclear; electrical and structural remodeling have emerged as key elements in the development of the atrial fibrillation substrate. In this work, we focus in electrical modeling, which includes changes in Ca^{2+} and K^+ currents leading to shortening of the action potential duration and loss of its rate-dependent adaptation. There are many experimental evidences that demonstrate the abnormal intracellular Ca^{2+} handling as a key mediator in atrial fibrillation pathophysiology. However, the system of Ca^{2+}-related anomaly related to occurrence and maintenance of atrial fibrilation is still poorly understood.

With the purpose of gaining insight into human atrial cell physiology many models of human atrial myocytes have been developed. However, non of these included detailed descriptions of calcium handling processes.

Recently, Grandi-Pasqualini-Bers [18] developed a model of the human ventricular myocyte action potential and Ca^{2+} transient. This model is developed within the framework of the Shannon-Bers rabbit ventricular model and based on experimental data obtained in human ventricular myocytes. A dominant novelty over prior human ventricular models is in robustly describing excitation-contraction coupling and the model was widely validated against a broad range of experimental data.

The Grandi-Pasqualini-Bers model is complex and well detailed, uses 38 state variables and 14 transmembrane currents; the fast Na^+ (I_{Na}) current, L-type Ca^{2+} (I_{CaL}), transient outward K^+ (I_{toL}), rapidly and slowly activating delayed rectifier K^+ (I_{Kr} and I_{Ks}, respectively), inward rectifier K^+ (I_{K1}), Na^+/Ca^{2+} exchanger (I_{NaCa}), Na^+/K^+ pump (I_{NaK}), sarcolemmal Ca^{2+} pump (I_{pCa}), background Na^+ (I_{bNa}), and background Ca^{2+} (I_{bCa}) currents. In addition to these, the model includes Ca^{2+}-activated Cl^- (I_{CaCl} or I_{to2}), plateau K^+ (I_{Kp}), and background Cl^- (I_{bCa}) currents, as well as fast and slow components of I_{to} and the Na^+ transport throught L-type Ca^{2+} channels. For more information about the variables and currents definition and formalization take a look into the supplementary material of the model [18].

Further, Grandi et al [11] developed a new atrial model, in the paper Human Atrial Action Potential and Ca^{2+} Model: Sinus Rhythm and Chronic Atrial Fibrillation and we use it for the purpose on this master thesis. This new human atrial model is based on the ventricular model and contains detailed electrophysiology and Ca^{2+} handling by implementing structural and ionic differences in atrial versus ventricular cells. The model differential equations were implemented in MATLAB

and taken from the repository CellML [30]. We remodel it additionally by adding the I_{SK} current to the code. Model solves Eq. (3); the total ion current flow I_m through the membrane over time (t) can be recapitulated into equation

$$I_m = I_{Na_{tot}} + I_{Ca_{tot}} + I_{Ca_{tot}} + I_{K_{tot}} + I_{Kur} + I_{SK3}. \tag{4}$$

The ODEs are solved numerically in MATLAB using a variable order solver (ode15s) which solved stiff differential equations and differential-algebraic equations (DAEs).

There exists different definitions of the I_{SK} current. The current can be written as:

$$I_{SK} = g_{SK} f(Ca)(V - E_K) \tag{5}$$

being g_{SK} conductance associated with the small conductance calcium-activated potassium current (measured in Siemens). E_k represents the Nernst potential for potassium and $f(Ca)$ gating variable defined as

$$f(Ca) = \frac{Ca^q}{K_{SK}^q + Ca^q} \tag{6}$$

In the model by Cha et al [25] some modifications of the previous formulation are done. Authors consider GHL formulation of the current;

$$I_{SK} = P_{SK} f(Ca) \frac{FV}{RT} \frac{[K]_i - [K]_0 exp(\frac{-FV}{RT})}{1 - exp(\frac{-FV}{RT})} \tag{7}$$

Also, a time depended calcium gate is introduced in the model by Engel et al [24] where the current is defined as

$$I_{SK} = g_{SK} f^2(Ca)(V - E_K) \tag{8}$$

and the gate satisfies equation

$$\frac{df}{dt} = \frac{f_\infty - f}{\tau_f} \tag{9}$$

and time is constatnt.

In our case, we introduce the I_{SK} current into model in the following form:

$$I_{SK} = g_{SK} z(V - E_K) \tag{10}$$

where z is a gating variable whose time dependence is described by

$$\frac{dz}{dt} = \frac{z_\infty - z}{\tau} \tag{11}$$

where

$$z_\infty = \frac{[Ca^{2+}]^2}{[Ca^{2+}]^2 + [K^+]^2}$$

and τ is a time constant associated with the activation or inactivation process. There exist some experiments proving that τ is calcium related also. However, from the experimental observations, this fact does not affect results much. Thus, taking into account the experimental observations, in our simulations $\tau = 5$ ms is fixed.

2.2 Validation of the model

In this subsection we want to validate the model in order to see effect of the introduced current.

The Figure 6 shows the effect of I_{SK} current in the Grandi model. The black line correspond to the action potential without the I_{SK} current, while the red and the blue lines corresponds to two I_{SK} currents with different conductance values: $\tilde{g} = 0.0015\ s^{-1}$ and $\tilde{g} = 0.003\ s^{-1}$, respectively. It is noticeable that the I_{SK} current is involved into shaping of AP. More precisely, I_{SK} current process shortening of the action potential in it's phase 3. Further, we observe shortening of the APD as the conductance becomes higher.

We are interested in study of the change of APD due to SK currents. To do so, it is necessary to calibrate the strength of this currents and find the best fitting model of the current corresponding to the experimental data. Following subsections are of this purpose.

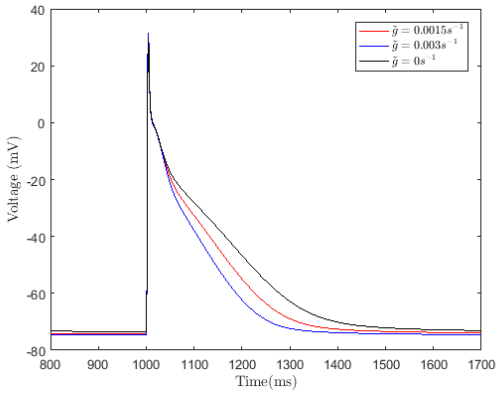

Figure 6: Effect of the I_{SK} current in Grandi model.

2.3 Rectification

Some studies have demonstrated that SK channels are expressed in human and mouse cardiac myocytes. More importantly, Zhang et all [12] found that SK current contributes significantly to the repolarization process in both mouse and human atria. Further studies in their laboratory revealed that different members of SK channels exist in human cardiac myocytes. Their studies have provided unique insights regarding the roles of these newly described channels in the heart. They directly tested the contribution of SK3 channels to the overall repolarization of atrial action potentials. They also demonstrate the important roles of SK3 channels towards the overall repolarization process of atrial myocytes. The details about experiment as well as Figure 7 can be found in paper by Zhang et all [12].

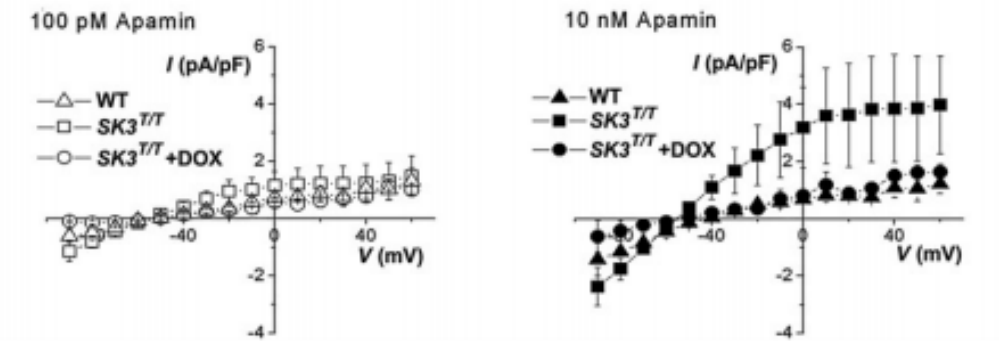

Figure 7: Whole-cell I_{KCa} currents have been recorded from mouse atrial myocytes. The apamin-sensitive current traces were obtained using digital subtraction; digital subtraction angiography (DSA) is a type of fluoroscopy technique used in interventional radiology to clearly visualize blood vessels in a bony or dense soft tissue environment. This figure is reproduced from the paper by Zhang et all [12].

From Figure 7 we obtain that above some value of voltage, the current saturates at a certain value. In order to define a more precise shape of the I_{SK} current, following the experimental results, rectification is done. Rectification of the current is shown in Figure 8. All the models presented in this paper are modeled by a linear dependent current of the form:

$$I_{SK} = \begin{cases} g_{SK} z(V - E_K) & \text{when } V < V_C \\ g_{SK} z(V_C - E_K) & \text{when } V > V_C. \end{cases}$$

The Nernst potential of the I_{SK} current, namely E_K, in our model is -82 mV. We are taking V_{C_1}, V_{C_2}, V_{C_3} the critical points of rectification that takes value -70 mV, -50 mV and -30 mV, respectively. Further, in our simulations is observed the wild type of the g_{SK3} value as well as overexpression of the wild type of g_{SK3}.

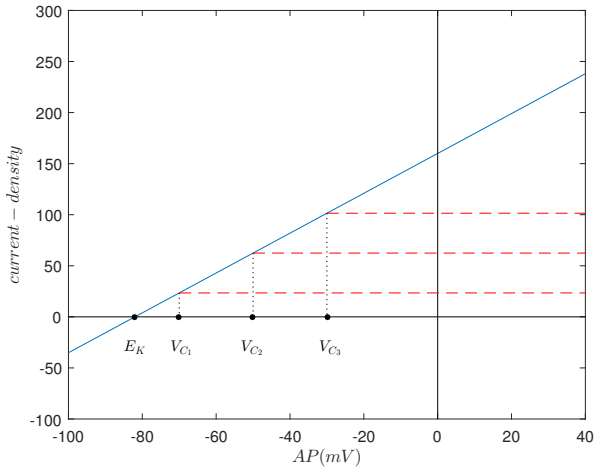

Figure 8: Model of the rectification for the tree different critical points V_{C_1}, V_{C_2}, V_{C_3}

.

2.4 Effect of SK current in the APD

We want to investigate how changes in SK3 physiology may affect the action potential. Our focus is on analysis in changes in the APD90, that is, the duration of action potential measured as the time it remains above 10% its minimum value, see Figure 9.

In order to investigate the behavior of SK channels, we considered the computational model described mathematically by Eq(10). The Figure 10 represents the duration of action potential evaluated for different values of g_{SK3} in order to calculate the correct g_{SK3} for each of the different models of current.

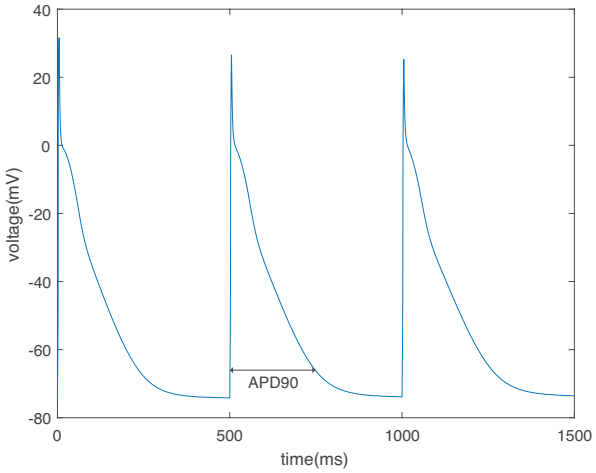

Figure 9: APD90 is a duration of the action potential mesured as the time it remains above 10% its minimum value.

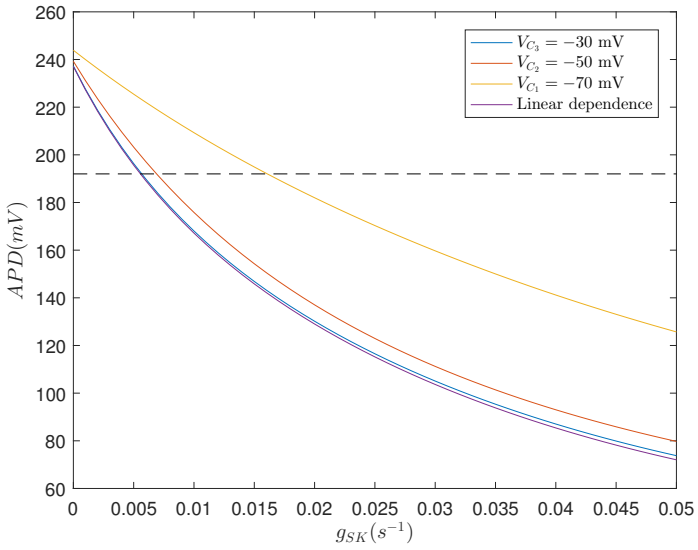

Figure 10: The action potential duration versus values of $\tilde{g}_{SK}$. The yellow line corresponds to the rectified model current for the value $V_{C_1} = -70$ mV. Red and blue lines corresponds to the rectified model current for the values $V_{C_2} = -50$ mV and $V_{C_3} = -30$ mV, respectively. Finally, the purple line corresponds to the linearly dependent current model. Dashed line present the decrease of about 20% of its maximum value for the $\tilde{g}_{SK3} = 0$.

We obtained a decrease in APD as the value of conductance increase for all the I_{SK3} models. Since the linear dependent current model does not differ noticeable from the rectified model current for the value of $V_{C_3} = -30$ mV, this case can be

Values of g_{SK3} (measured in Siemens)			
	linear	$V_c = -50$ mV	$V_c = -70$ mV
original	0.05	0.05	0.05
wild type	0.005	0.006	0.014
over expression	0.01	0.012	0.028

Table 1: Table with the corresponding value of g_{SK3} for each of the different current model.

neglected. We will focus in the rectified model with $V_{C_1} = -70$ mV, $V_{C_2} = -50$ mV and the linear dependence current model.

There exist several experiments studying reduction of APD due to the presence of the I_{SK} current. In these papers is represented the standard behavior of I_{SK} using the wild type expression of g_{SK} and apamin blocked I_{SK} current. The difference between them corresponds to the effect of the I_{SK} current. The value of g_{SK} is selected to reproduce these variations. Effect of the standard I_{SK} current on the APD shows decrease of about 20 in percentage. That is why we are taking values of g_{SK} that are about 20% below its maximum value. Therefore, in the $V_{C_1} = -70$ model we are taking the $\tilde{g} = g_{SK3}/Cm$ value equal to 0.0014 s^{-1}, in the $V_{C_2} = -50$ mV it is $\tilde{g}_{SK3} = 0.0006$ s^{-1} and for the linear case $\tilde{g}_{SK3} = 0.0005$ s^{-1}. The summary of the g_{SK3} value for each current model is presented in Table 1. The original value is the $\tilde{g}_{SK3}$ value initially incorporated into the Grandi model.

Further, we can see that as the absolute value of the critical point is larger, the conductance needs to be larger as well. This fact will be important while studying the effect of SCR; the larger conductance is, the bigger effect on SCR is. That is why the model $V_{C_1} = -70$ mV is the preferable one.

2.5 Deterministic SCR

Deterministic SCR is modeled by fixing values of wild type expresion and overexpression of the conductance for each of the three considered current models. We will remodel opening of RyRs receptor to produce spontaneous calcium release from the SR. The RyR channel is considered to be open when its opening probability P_O is equal to 1. In order to produce SCR we changed the opening rate. Simplification of the dynamics of the RyRs can be schematically showed, see Figure 11. RyRs have four possible states, open (O), closed (C), and two inactivated states (I_1, I_2). Their probability rate equations are

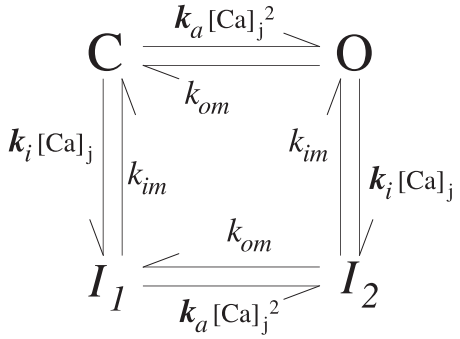

Figure 11: Dynamics and the probabilities states of the RyRs.

$$
\begin{aligned}
\frac{dP_C}{dt} &= k_{im}P_{I_1} - k_i c_j P_C - k_a c_j^2 P_C + k_{om}P_O,\\
\frac{dP_O}{dt} &= k_a c_j^2 P_C - k_{om}P_O - k_i c_j P_O + k_{im}P_{I_2},\\
\frac{dP_{I_1}}{dt} &= k_{om}P_{I_1} - k_a c_j^2 P_{I_1} - k_{im}P_{I_1} + k_i c_j P_C,\\
\frac{dP_{I_2}}{dt} &= k_i c_j P_O - k_{im}P_{I_2} - k_{om}P_{I_2} - k_a c_j^2 P_{I_1}.
\end{aligned}
$$

We model the SCR increasing the opening probability k_a of the RyRs receptors by a given factor $aSCR$ at a given time T_{SCR}. Then we study the depolarization as a function of these two parameters $aSCR$ and T_{SCR}.

3 Results

In this section we perform the simulations based on the remodeled Grandi model. Firstly, we produce the calcium release at the certain time T_{SCR} with a certain strength $aSCR$ in order to obtain EAD and DAD. First we show the concentration of the intracellular calcium and transmembrane potential, in the case of an SCR event. Simulations are done for the two models, $V_{C_1} = -70$ mV and $V_{C_2} = -50$ mV in both cases of the pacing period, $T = 1000$ ms and $T = 500$ ms. Secondly, phase diagram plots show the depolarized or non-depolarized areas for each of the models. Lastly, to see effect of the SK current more clearly, there are plots with contour lines separating these regions for each conductance in model of $V_{C_1} = -70$ mV and $V_{C_2} = -50$ mV.

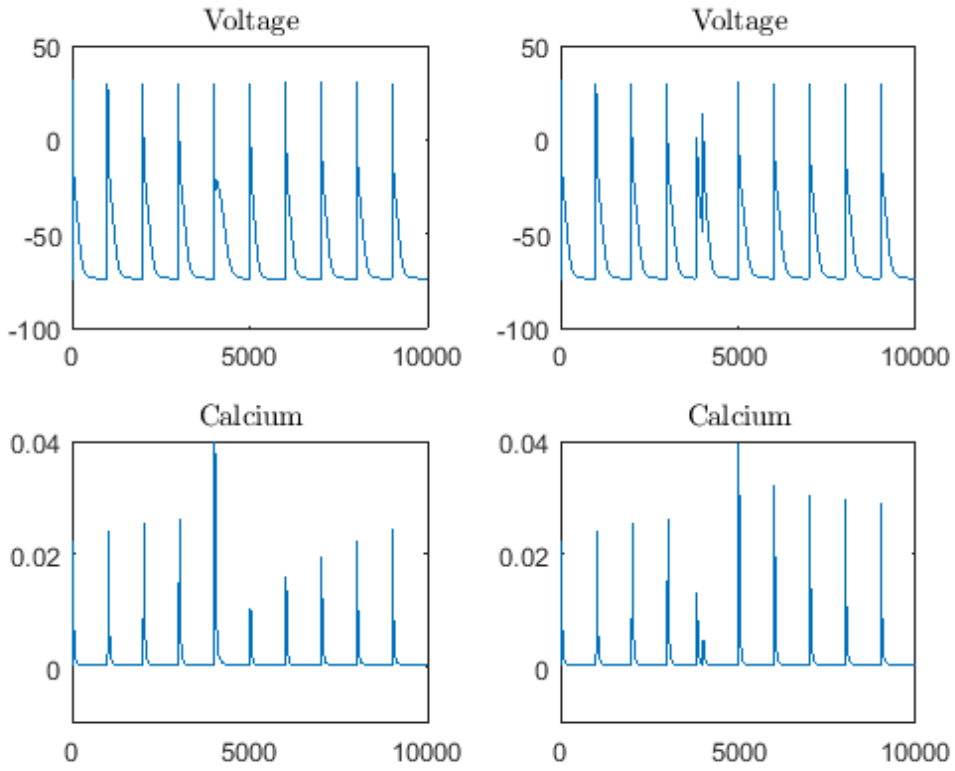

Figure 12: Representation of the failed (top and bottom left panel) and succeeded (top and bottom right panel) EAD.

The Figure 12 shows the failure and success of EAD in the model $V_{C_1} = -70$ mV at a pacing period $T = 1000$ ms. We fixed the time at which the SCR is produced. The top and bottom left panels shows failure to produce an EAD because the strength of the current I_{SK} is not strong enough to reach the threshold

for excitation. Here the time at which the RyR receptors are opened is $T_{SCR} = 3800$ ms and the strength is $aSCR = 24$. Due to the increase of the calcium concentration at this time T_{SCR} (see bottom left panel), in the top left panel we observe the slight increase of voltage in the phase 3 of the action potential. As a consequence, the concentration of calcium in the next spike is lowered. The right two panels represent EAD. In this case the time of SCR is $T_{SCR} = 3800$ ms but the strength of the current is $aSCR = 28$. There is an evident drop of the calcium concentration at the time T_{SCR} that leads to a huge increase of calcium in the next spike of the action potential.

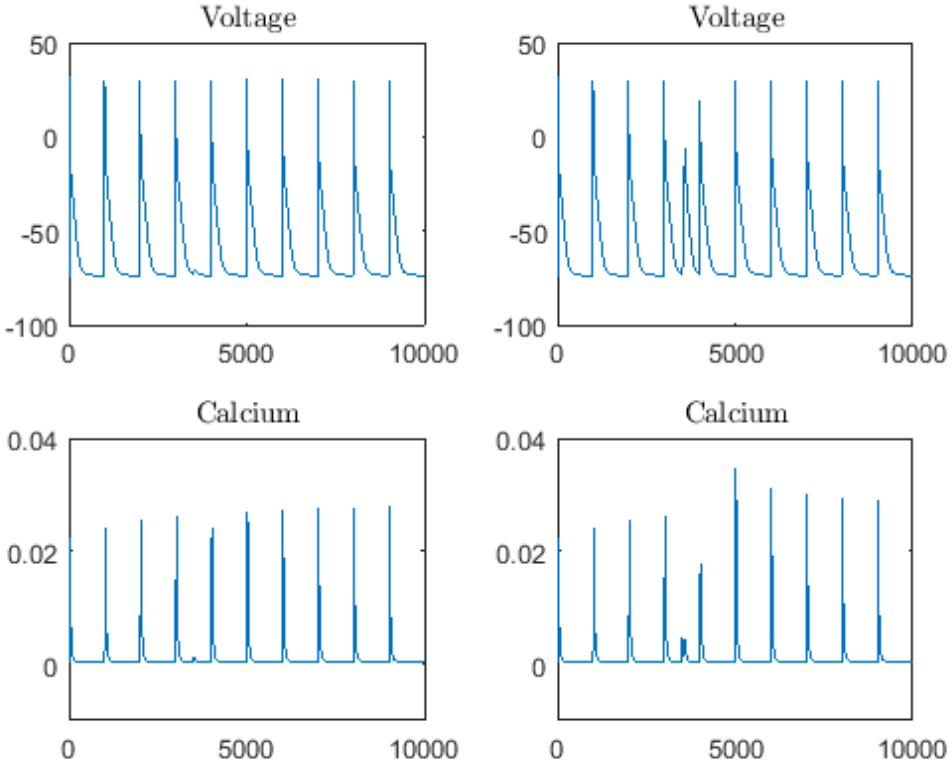

Figure 13: Representation of the failed (top and bottom left panel) and succeeded (top and bottom right panel) DAD in the model $V_{C_1} = -70$ mV.

All plots presenting the EAD and the DAD are based on the same concept as the previous plot. By changing the strength of the SK current and depending on the chosen time, either a EAD or DAD is produced.

In Figure 13, that shows the failure and success of DAD in the model $V_{C_1} = -70$ mV at a pacing period $T = 1000$ ms, we fixed the time $T_{SCR} = 3500$ ms at which SCR is produced. The top and bottom left panels show failure to produce the DAD; with $aSCR = 24$. The action potential at this time shows a slight

decrease, as well as the concentration of the calcium increases very little. On the other hand, the right two panels represent a DAD. In this case the rate of RyR opening is increased by a factor $aSCR = 30$. As the action potential reaches the threshold, the "new" spike takes a place between the two "ordinary" spikes causing the entering the calcium into the cytosol. Therefore, the concentration of calcium in the next spike is lower due to the channel opening and then, the concentration of the calcium in the next spike is greater than usually.

We have done the simulation in order to observe the EAD and DAD in the rectified model $V_{C_2} = -50$ mV as well. The pacing period T in this model was $T = 500$ ms.

The Figure 14 shows the SRC fails and success to produce an early afterdepolarisation. The fixed time at which we decide to produce SCR is $T_{SCR} = 3250$ ms. The increase in RyR opening rate at the top and bottom left panel is $aSCR = 22$, and therefore it shows failure produce the EAD. At the same time T_{SCR}, but with $aSCR = 30$, spontaneous calcium release succeeds to produce the EAD. Here we can see how the changes in the concentracion of intracellular calcium can have noticeable impact on the shaping of the action potential.

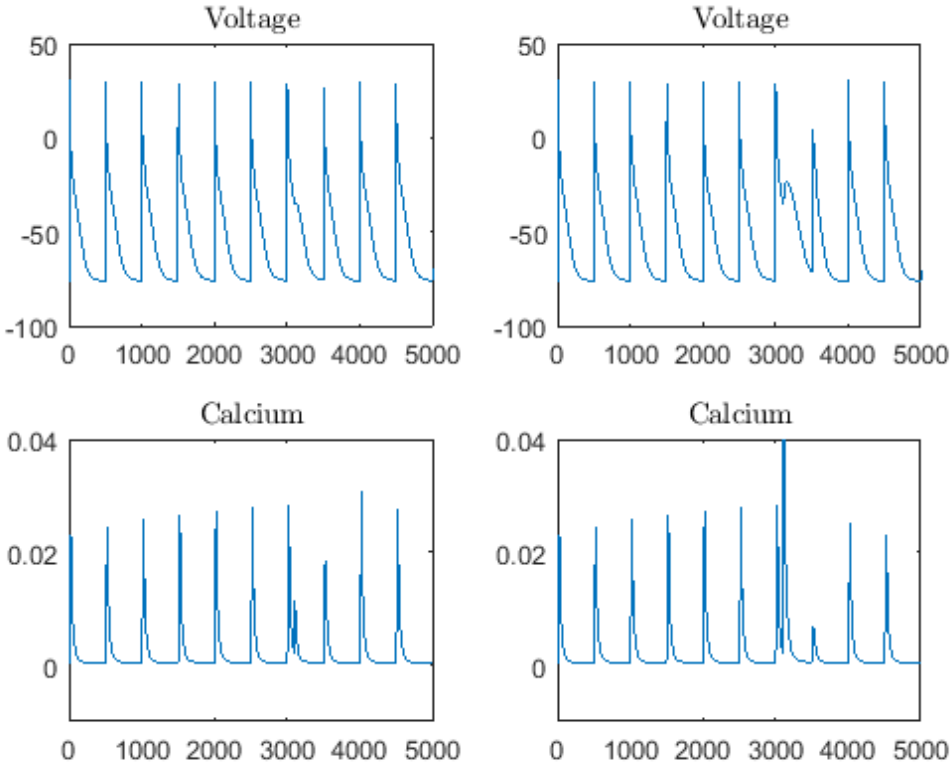

Figure 14: Shows the failed (top and bottom left panel) and succeeded (top and bottom right panel) EAD due to the SCR in the model $V_{C_1} = -50$ mV.

Lastly, Figure 15 show the failure and success of DAD. The fixed time is $T_{SCR} =$ 3350 ms. The top and bottom left panels shows failure to produce the DAD; when $aSCR = 22$. The right two panels represent DAD with $aSCR = 28$. Similarly as in previous cases, increased calcium concentration has a huge effect in the phase 4 of the action potential.

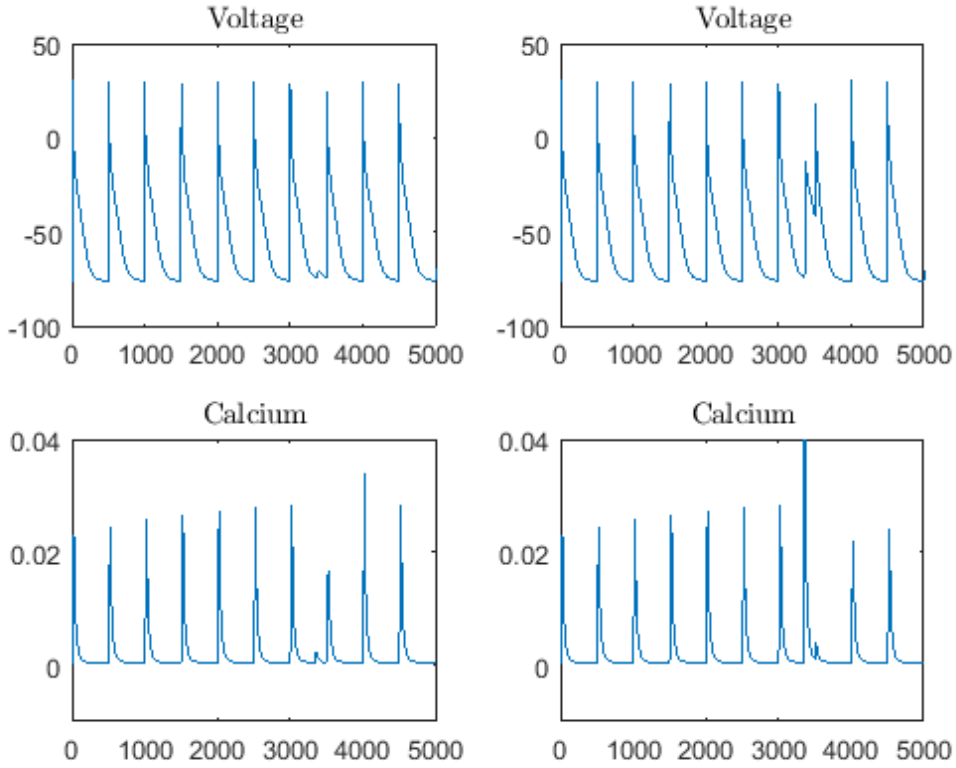

Figure 15: Present when the SCR failed to produce the DAD (top and bottom left panel) and when it succeed to producethe DAD (top and bottom right panel).

In Figures 16, 17, and 18 we show the phase diagram plots with lines separating areas with delayed depolarization (area of the colour blue) and without delayed depolarization (area corresponding to the yellow colour) for the three different models and different values of conductance.

The Figure 19 shows contour lines for the wild type of conductance $\tilde{g} = 0.0014$ s^{-1} and overexpression of the conductance $\tilde{g} = 0.0028$ s^{-1} as well as conductance equal to zero in the model $V_{C_1} = -70$ mV. In this figure it is clearly seen that the effect of the SK current in not linear with the increase of the conductance.

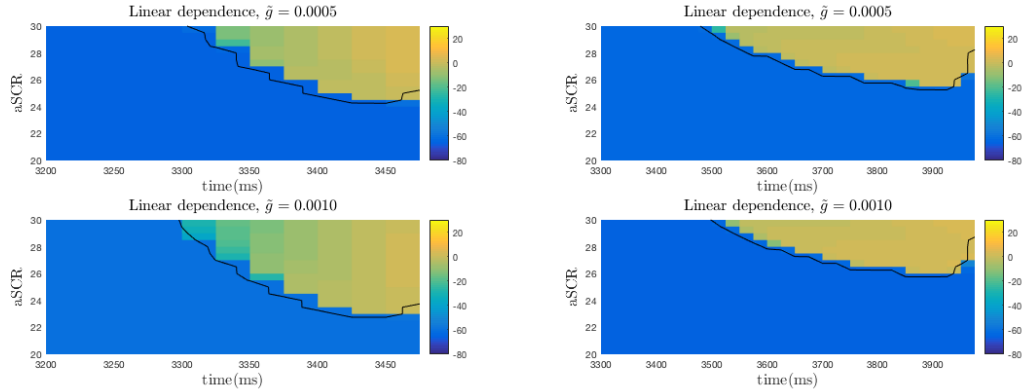

Figure 16: The left panels correspond to a pacing period of $T = 500$ms, while the right panels to $T = 1000$ ms. Top left panel corresponds to phase diagram plot of the linearly dependent current model and wild type conductance expression $\tilde{g} = 0.0005\ s^{-1}$ while bottom panel represents overexpressed conductance value $\tilde{g} = 0.0010\ s^{-1}$. The same values of $\tilde{g}$ is presented in the top and bottom right panels, but in case of time period $T = 500$ ms. All the panels consider the same range of increase in RyR opening that is $aSCR \in [20, 30]$. In the case $T = 500$ ms time range for spontaneous calcium release is $T_{SCR} \in [3200, 3499]$ while in the case $T = 1000$ ms, $T_{SCR} \in [3300, 3999]$.

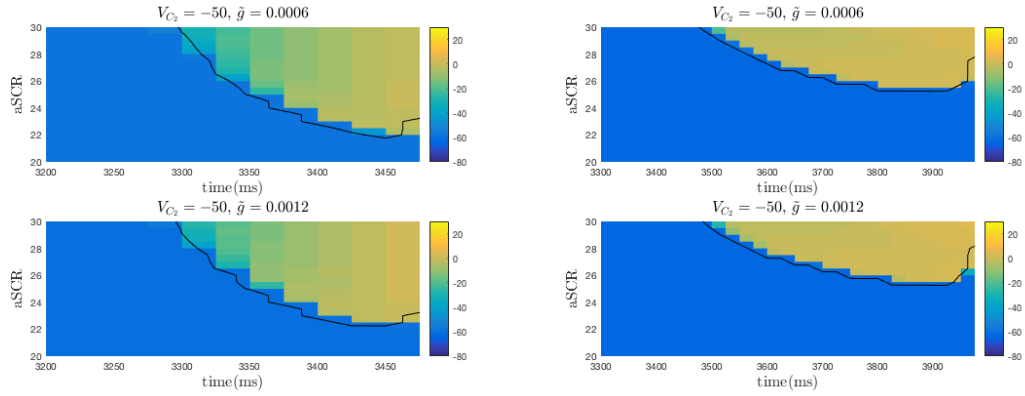

Figure 17: Top left panel corresponds to phase diagram plot of the rectified current model $V_{C_2} = -50$ mV and wild type conductance expression $\tilde{g} = 0.0006\ s^{-1}$ while bottom panel represents overexpressed conductance value $\tilde{g} = 0.0012\ s^{-1}$. The left panels correspond to a pacing period of $T = 500$ms, while the right panels to $T = 1000$ms. The same values of $\tilde{g}$ is presented in the top and botom right panels, but in case of time period $T = 500$ ms. All the panels consider the same range of increase in RyR opening that is $aSCR \in [20, 30]$. In the case $T = 500$ ms time range for spontaneous calcium release is $T_{SCR} \in [3200, 3499]$ while in the case $T = 1000$ ms, $T_{SCR} \in [3300, 3999]$.

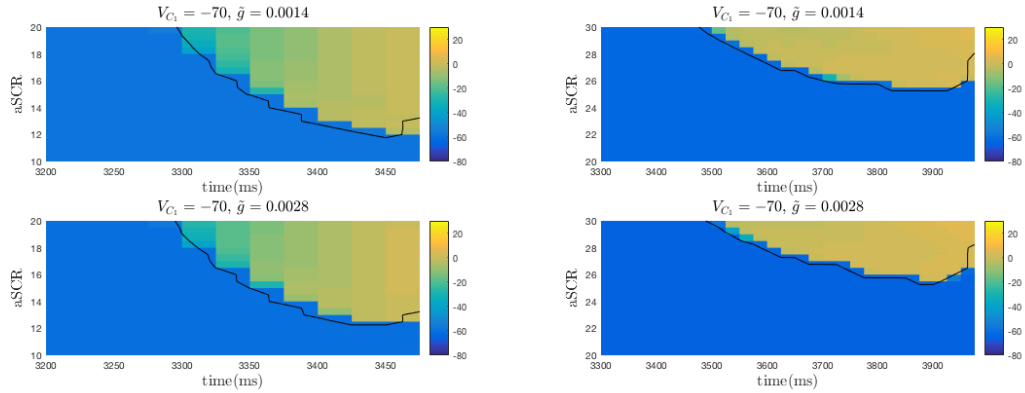

Figure 18: Top left panel corresponds to phase diagram plot of the rectified current model $V_{C_2} = -70$ mV and wild type conductance expression $\tilde{g} = 0.0014\ s^{-1}$ while bottom panel represents overexpressed conductance value $\tilde{g} = 0.0028\ s^{-1}$. The left panels correspond to a pacing period of $T = 500$ms, while the right panels to $T = 1000$ms. The same values of $\tilde{g}$ is presented in the top and botom right panels, but in case of time period $T = 500$ ms. All the panels consider the same range of increase in RyR opening that is $aSCR \in [20, 30]$. In the case $T = 500$ ms time range for spontaneous calcium release is $T_{SCR} \in [3200, 3499]$ while in the case $T = 1000$ ms, $T_{SCR} \in [3300, 3999]$.

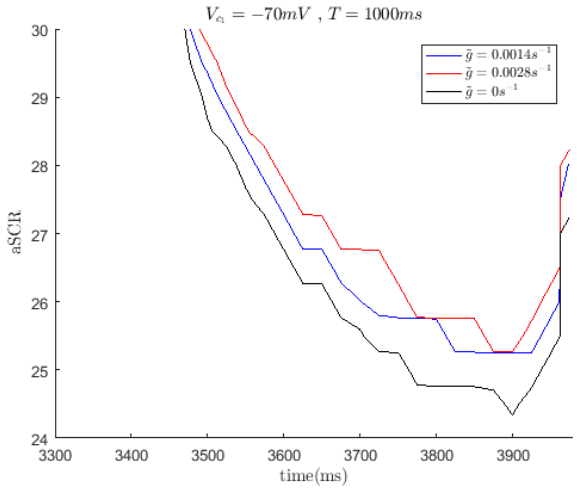

Figure 19: Contour lines for different conductance values in the model $V_{C_1} = -70$ mV and $T = 1000$ ms.

Next Figure 20 represents contour lines in the model $V_{C_2} = -50$ mV for the wild type value of conductance $\tilde{g} = 0.0006\ s^{-1}$ and overexpression of the conductance $\tilde{g} = 0.0012\ s^{-1}$ as well as conductance equal to zero. Comparing these figures with the figure of the $V_{C_1} = -70$ mV model where the $T = 1000$ ms, we can conclude

that the effect is larger in the case of pacing the action potential with the larger pacing time T.

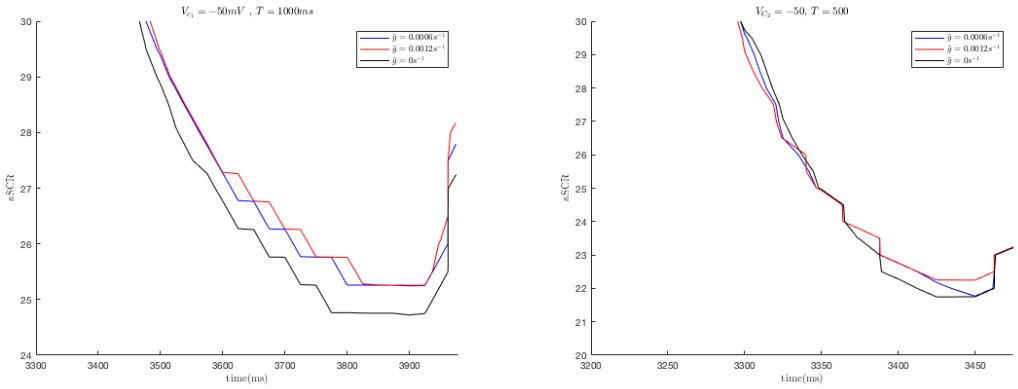

Figure 20: Contour lines for different conductance values in the model $V_{C_1} = -50$ mV. The left panel corresponds to the case when $T = 1000$ ms while the right one corresponds to the case $T = 500$ ms.

4 Discussion and conclusions

In this work we have been studying the anatomy of the heart and basic cardiac cellular electrophysiology. We introduce the mechanism underlying the contraction of the heart as well as the family of the small-conductance Ca^{2+}-activated potassium channels. In order to study the effect of SK current, we remodel the well established Grandi model introducing the SK current into the code. Based on the experimental data, we rectified the current to calibrate the strength of this current. Presenting the duration of the action potential evaluated for different values of g_{SK3}, we saw the decrease in APD as the value of conductance increases. However, we did not do simulations for the original values of conductance because the results do not agree the experimental data. As it can be seen in the Figure 10, the APD in this case in much lower than the rectified models than we examine. Then, we studied the effect of the SK current on depolarization. Further, we set a fixed release of calcium at different times producing the EADs or DADs.

The role of the SK channels and possible functional SK current in the cardiac electrophysiology in recent years has been debated and the pro/anti arrhythmic effect of the SK channels has been of particular controversy.

In this paper we performed numerical simulations of whole-cell atrial myocyte. There is noticeable effect of the I_{SK} in the APD as we saw in Figure 6. Also, we observe an anti arrhythmic effect of the SK current during spontaneous calcium release events. However, the results presented in this thesis imply that the anti arrhythmic mechanism generated by the SK current may not play a mayor role under realistic conditions. The current seems to not be "strong" enough to prevent most cased of SCR induced depolarizations. Therefore, our results do not support the idea of developing SK channel blockers as a new therapeutic strategy in the treatment of atrial fibrillation. It is possible that the real form of the SK current has a more complex dependence on calcium concentration and its regulation than the Grandi model considers. That may be one of the reasons of not observing such a big effect of SK current as the experimental data indicate.

The potentially interesting expansion of this work would be to perform the stochastic events of calcium release; random distribution in time and strength of the release. Considering the uniform, Gaussian or Poisson probability distributions, it would be interesting to calculate the statistics of induced repolarizations with and without the SK current.

References

[1] Andrew J. Pullan, Leo K. Cheng, Martin L. Buist. 'Mathematical modelling the electrical activity of the heart: from cell to body surface and back again', *World Scientific Publishing,* 1–147, 2005.

[2] A. Peñaranda, I. R. Cantalapiedra, E. Alvarez-Lacalle, B. Echebarria. 'Electrophysiological effects of small conductance Ca^{2+}'-activated K^+, channels in cardiac myocytes *World Scientific Publishing,* , 1–15, 2017.

[3] L. Skibsbye. Antiarrhythmic principle of SK channel inhibition in atrial fibrillation. *Channels*, 57:672–81, 2011.

[4] J.P. Adelman, J. Maylie, P. Sah. Small-conductance Ca^{2+}-activated K^+ channels: form and function. *Annu Rev Physiol*, 74:245–269, 2012.

[5] M. Kohler, B. Hirschberg, C.T. Bond, J.M. Kinzie, N.V. Marrion, J. Maylie, J.P Adelman. Small-conductance, calcium-activated potassium channels from mammalian brain. *Science*, 273:1709–1714, 1996.

[6] I. M. Bonilla, V. P. Long III, P. Vargas-Pinto, P. Wright, A. Belevych, Q. Lou, K. Mowrey, J. Yoo, P. F. Binkley, V. V. Fedorov, et al. 'Calcium-activated potassium current modulates ventricular repolarization in chronic heart failure', *PloS one*, 9(10):e108824, 2014.

[7] S. K. Chua, P. C. Chang, M. Maruyama, I. Turker, T. Shinohara, M. J. Shen, Z. Chen, C. Shen, M. Rubart-von der Lohe, J. C. Lopshire, et al. 'Small-conductance calcium-activated potassium channel and recurrent ventricular fibrillation in failing rabbit ventricles', *Circulation research*, 108(8):971–979, 2011.

[8] J. G. Diness, Bo H. Bentzen, U. S. Sørensen, M. Grunnet. 'Role of Calcium-activated Potassium Channels in Atrial Fibrillation Pathophysiology and Therapy', *J Cardiovasc Pharmacol*, 66(5):441–448, 2015.

[9] T. Yu, C. Deng, R. Wu, H. Guo, S. Zheng, X. Yu, Z. Shan, S. Kuang, Q. Lin. 'Decreased expression of small-conductance Ca^{2+}-activated K^+ channels SK1 and SK2 in human chronic atrial fibrillation?, *Life sciences*, 90(5):219–227, 2012.

[10] T. Y. Ling, X. Wang, Q. Chai, T.-W. Lau, C. M. Koestler, S. J. Park, R. C. Daly, K. L. Greason, J. Jen, L.-Q. Wu, et al. 'Regulation of the SK3 channel by microrna-499potential role in atrial fibrillation', *Heart Rhythm*, 10(7):1001–1009, 2013.

[11] E. Grandi, S. V. Pandit, N. Voigt, A. J. Workman, D. Dobrev, J. Jalife, D. M. Bers. 'Human Atrial Action Potential and Ca^{2+} Model: Sinus Rhythm and Chronic Atrial Fibrillation', *Circulation Research*, 109:1055-1066, 2011.

[12] X.D. Zhang, V. Timofeyev, N. Li, R. E. Myers1, D.-M. Zhang, A. Singapuri, V. C. Lau, C. T. Bond, J. Adelman, D. K. Lieu, N. Chiamvimonvat. 'Critical roles of a small conductance Ca^{2+}-activated K^+ channel (SK3) in the repolarization process of atrial myocytes', *Cardiovascular Research*, 101:317–325, 2014.

[13] H.M. Lo, F.Y. Lin, J.L. Lin, K.L. Hsu, F.T. Chiang, C.D. Tseng, Y.Z. Tseng. 'Impaired cardiac performance relating to delayed left atrial activation after atrial compartment operation for chronic atrial fibrillation Pacing', *Clin. Electrophysiol.*, 22:379-381, 1999.

[14] D.M. Bers. 'Cardiac excitation–contraction coupling', *Nature*, 415:198-205, 2002.

[15] A. L. Blatz, K. L. Magleby. 'Single apamin-blocked Ca-activated K+ channels of small conductance in cultured rat skeletal muscle', *Nature*, 323(1):718–720, 1986.

[16] P. T. Ellinor, K. L. Lunetta, C. M. Albert, N. L. Glazer, M. D. Ritchie, A. V. Smith, D. E. Arking, M. Muller-Nurasyid, B. P. Krijthe, S. A. Lubitz, et al. 'Meta-analysis identifies six new susceptibility loci for atrial fibrillation', *Nature genetics*, 44(6):670–675, 2012.

[17] L. Hove-Madsen, A. Llach, A. Bayes-Genís, S. Roura, E. Rodriguez Font, A. Arís, J. Cinca. 'Atrial Fibrillation Is Associated With Increased Spontaneous Calcium Release From the Sarcoplasmic Reticulum in Human Atrial Myocytes', *Circulation*, 110:1358-1363, 2004.

[18] E. Grandi, F.S. Pasqualini, D. M. Bers. 'A novel computational model of the human ventricular action potential and Ca transient', *Journal of Molecular and Cellular Cardiology*, 48:112-121, 2010.

[19] G. Ikonnikov, D. Yelle. 'Physiology of cardiac conduction and contractility', *McMaster Pathophysiology Review*, 40(11):1053-64, 1993.

[20] Y. Xu, D. Tuteja, Z. Zhang, et al. 'Molecular identification and functional roles of a Ca^{2+}-activated K^+ channel in human and mouse hearts', *J Biol Chem*, 278:49085–49094, 2003.

[21] N. Chiamvimonvat, D. Tuteja, D. Xu, V. Timofeyev, L. Lu, D. Sharma, Z. Zhang, Y. Xu, L. Nie, A. E. Vázquez, J. Nilas Young, K. A. Glatter. 'Differential expression of small-conductance Ca^{2+}-activated K^+ channels SK1,

SK2, and SK3 in mouse atrial and ventricular myocytes', *AJP-Heart and Circ*, 289:6, 2005.

[22] N. Ozgen, W. Dun, E. A. Sosunov, et al. 'Early electrical remodeling in rabbit pulmonary vein results from trafficking of intracellular SK2 channels to membrane sites', *Cardiovasc Res*, 75:758-769, 2007.

[23] N. Chiamvimonvat, D. Tuteja, D. Xu, V. Timofeyev, L. Lu, D. Sharma, Z. Zhang, Y. Xu, L. Nie, A. E. Vázquez, J. Nilas Young, K. A. Glatter. 'Ablation of a Ca^{2+}-activated K^+ channel (SK2 channel) results in action potential prolongation in atrial myocytes and atrial fibrillation', *AJP-Heart and Circ*, 587:1087–1100, 2009.

[24] J. Engel, H. A. Schultens, D. Schild. 'Small conductance potassium channels cause an activity-dependent spike frequency adaptation and make the transfer function of neurons logarithmic', *Biophysical journal*, 76(3):1310–1319, 1999.

[25] C. Y. Cha, Y. Nakamura, Y. Himeno, J. Wang, S. Fujimoto, N. Inagaki, Y. E. Earm, A. Noma. 'Ionic mechanisms and Ca^{2+} dynamics underlying the glucose response of pancreatic b cells: a simulation study', *The Journal of general physiology*, 138(1):21–37, 2011.

[26] S. Rafizadeh, Z. Zhang, R.L. Woltz, et al. 'Functional interaction with filamin A and intracellular Ca^{2+} enhance the surface membrane expression of a small-conductance Ca^{2+}-activated K^+ (SK2) channel', *Proc Natl Acad Sci USA*, 111:9989–9994, 2014.

[27] Y.H. Mu, W.C. Zhao, P. Duan, Y. Chen, W.D. Zhao, Q. Wang, H.Y. Tu, Q. Zhan. 'RyR2 modulates a Ca^{2+}-activated K^+ current in mouse cardiac', *myocytesPLoS One*, 9:e94905, 2014.

[28] N. Li, V. Timofeyev, D. Tuteja, et al. Ablation of a Ca^{2+}-activated K^+ channel (SK2 channel) results in action potential prolongation in atrial myocytes and atrial fibrillation', *J Physiol. Mar* 587:1087–1100, 2009.

[29] C.H. Hsueh, P.C. Chang, Y.C. Hsieh, T. Reher, P.S. Chen, S.F. Lin. 'Proarrhythmic effect of blocking the small conductance calcium activated potassium channel in isolated canine left atrium', *Heart Rhythm*, 10:891–898, 2013.

[30] E. Grandi, S. V. Pandit, N. Voigt, A. J. Workman, D. Dobrev, J. Jalife, D. M. Bers. 'Human Atrial Action Potential and Ca^{2+} Model: Sinus Rhythm and Chronic Atrial Fibrillation', https://models.physiomeproject.org/cellml